

The mineralogy and geochemistry of Permian lateritic ores in east of Shahindezh, West-Azarbaidjan province

A. Abedini^{1*}, A.A. Calagari²

1-Geology Department, faculty of Sciences, Urmia University, Urmia, Iran.

2- Geology Department, Faculty of Natural Sciences, Tabriz University, Tabriz, Iran.

(Received: 18/4/2011, in revised form: 23/7/2011)

Abstract: East of Shahindezh (south of West Azarbaidjan province), as a part of Irano-Himalayan karst bauxite belt, comprises discontinuous layers and lenses of bauxite, laterite, and kaolin within the Ruteh carbonate formation (Middle- Upper Permian). The XRD analyses show that the lateritic ores have rather simple mineralogy, and consist of hematite, boehmite, and kaolinite as major phases accompanied by minor phases such as goethite, montmorillonite, diaspore, illite, chlorite, and rutile. According to petrographical considerations, it can be deduced that the ores have polycyclic nature and their evolution being largely affected by the function of diagenetic and epigenetic processes. Petrographical features along with mineral assemblages reveal that the lateritic ores were deposited almost in a vadose environment. Based on chemistry of major elements, the ores are categorized into three types; (1) bauxitic ferrite, (2) laterite, and (3) ferritic laterite. Distribution pattern of REEs normalized to chondrite displays a low degree of differentiation between LREEs and HREEs and also a weak negative anomaly for Eu during the lateritization processes. These features along with field relations and concentration values of Al, Ti, and Zr indicate a diabasic protolith for the ores. Consideration of Ce and Eu anomalies unveil that the intensity of lateritization is directly related to the pH increase of drained water, Eh variations, and fluctuation of water table. Results from geochemical data have furnished compelling evidence that buffering of underground descending acidic weathering solutions, dissimilarities in degree of resistance against weathering among primary minerals, discrepancies in degree of stability of complexing legands, and chemical characteristics of elements are four key controlling factors for the distribution and behavior of major, minor, trace, and rare earth elements during lateritization in east of Shahindezh.

Keywords: *West-Azarbaidjan; Shahindezh; lateritization; protolith; distribution pattern of elements.*

Introduction

The study area is located in ~8 km east of Shahindezh, south of West-Azarbaidjan, and extends from 46°, 39', 28" to 46°, 44', 46" east longitude and from 36°, 37', 41" to 36°, 42', 52" north latitude (Fig.1). This area, based upon world's residual deposits [1], is reckoned a part of Irano-Himalayan karst bauxite belt. In recent years a lot of studies have been done on exploration and recognition of appropriate laterite, bauxite, and

kaolin within the Ruteh carbonate formation in this area by many researchers. Alavi-Naini et al. [2] and Kholghi Khasraghi et al. [3] were the first workers who prepared the geologic maps of Takab (1:250000) and Shahindezh (1:100000), respectively and in their attempts they also briefly studied some samples from this type of mineralization in the study area. Further academic works in the form of M.Sc. and Ph.D. theses projects by Etemadi [4], Abedini [5], and Abedini

* Corresponding author, Tel: (0441) 2972134, Fax: (0441) 2776707, Email: a.abedini@urmia.ac.ir

et al. [6] have been implemented to put special emphasis on characteristics of bauxite deposits from economic geology standpoint in the area. The previous works were focused principally on geology of bauxites, but the mineralogy and geochemistry of elements within laterites have not been earnestly noted. In this article, however, it has been endeavored by using petrographical, mineralogical, and geochemical data to focus chiefly on genetic aspects of lateritic mineralization, petrographic characteristics, origin, factors controlling distribution and behavior of major, minor, trace, and rare earth elements during lateritization, and physico-chemical conditions ruling in depositional environment.

Methods of investigation

This study was fulfilled in two parts, (1) field and (2) laboratory. The field works include selection of traverses across the strike of horizon containing the

ores in order to estimate the ore geometry and field relations among lithologic units. Representative samples of lateritic ores (#40) and igneous rocks (#5) which are presumed to be genetically related to lateritization were taken. The lab works began with preparation of thin-polished sections (20 samples) for petrographical examinations. X-ray Diffraction (XRD) method was employed for identification of unknown mineral phases (5 samples) and their semi-quantitative values in X-ray lab at GSI (Geological Survey of Iran). Finally, selective samples of the lateritic ores (#10) and the igneous rocks (#2) were analyzed for major, minor, trace, and rare earth elements by utilizing ICP-AES and ICP-MS methods in laboratories at ALS-Chemex, Canada. Loss on ignition (LOI) was measured by weighing the samples before and after one hour of heating at 1000°C. The analytic results from XRD, ICP-AES, and ICP-MS are listed in tables 1 and 2.

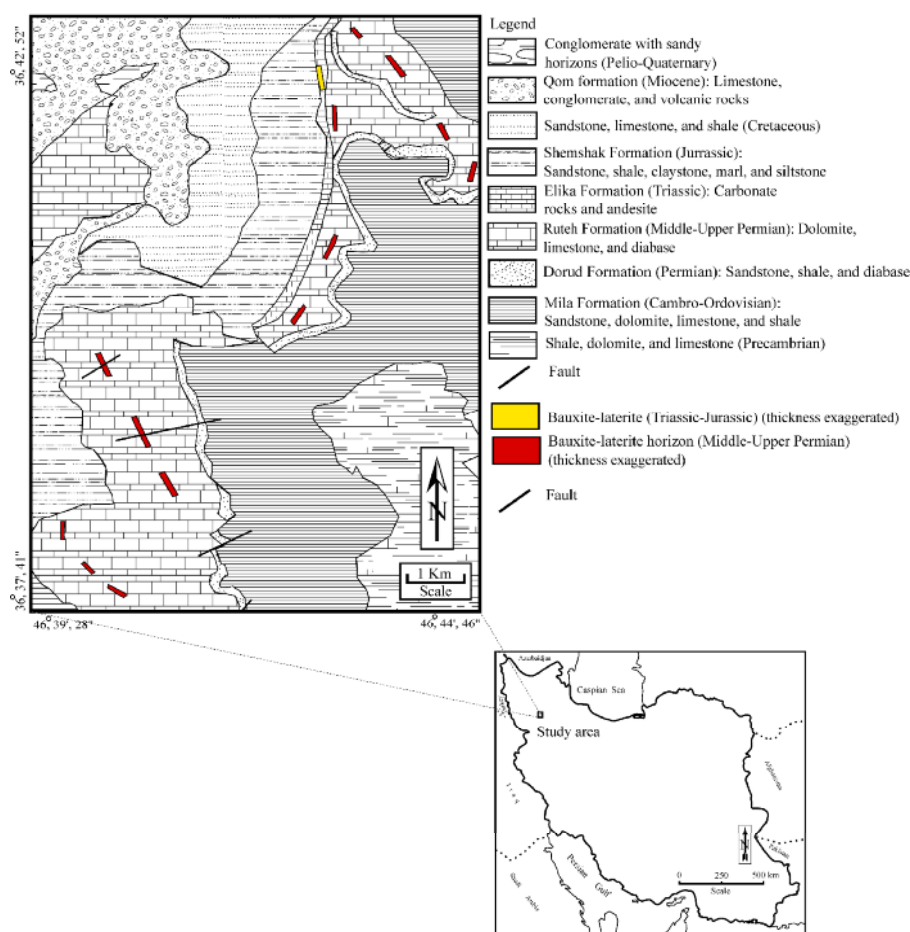


Fig.1 Geologic map of studied area (after [3]) and the position of the lateritic layers and lenses within the carbonate rocks of Ruteh Formation.

Table 1 Semi-quantitative values of various kinds of minerals in the lateritic ores in the studied area.

Sample	Diaspore	Boehmite	Kaolinite	Hematite	Goethite	Montmorillonite	Illite	Chlorite	Rutile
L-1	—	29.4	—	59.6	8.4	0.3	—	—	2.3
L-3	—	10.7	35.7	39.8	6.5	0.9	3.5	0.3	2.6
L-5	9.8	20.6	25.8	33.2	5.6	0.5	2.2	—	2.3
L-7	2.4	21.6	17.4	55.5	—	0.6	—	—	2.5
L-9	4.1	19.9	23.1	33.6	—	6.2	7.8	2.5	2.8

Table 2 Quantitative values of major, minor, trace, and rare earth elements (analyzed by ICP-AES and ICP-MS methods) as well as LOI in the lateritic ores and diabasic rocks in the studied area.

	D-1	D-2		L-1	L-2	L-3	L-4	L-5	L-6	L-7	L-8	L-9	L-10
	Diabase			Lateritic ores									
SiO ₂ wt%	48.9	49.6		1.3	24.2	21.2	28.4	15.1	18.5	8.9	30.2	28.1	13.7
Al ₂ O ₃	15.1	14.9		17.4	19.7	19.25	19.3	19.51	18.44	21.14	22.2	21.7	19.21
Fe ₂ O ₃	14.5	14.5		69.4	43.2	46.4	39.7	53.2	49.95	57.8	35.2	35.7	53.45
CaO	6.62	6.78		0.12	0.17	0.14	0.15	0.13	0.13	0.14	0.12	0.18	0.14
MgO	4.98	4.59		0.02	0.18	0.13	0.14	0.12	0.16	0.11	0.14	0.18	0.14
Na ₂ O	3.98	3.82		0.04	0.12	0.11	0.14	0.07	0.12	0.07	0.16	0.79	0.09
K ₂ O	1.62	1.84		0.05	0.49	0.41	0.53	0.25	0.36	0.15	0.6	0.91	0.25
TiO ₂	2.04	2.05		2.51	2.59	2.75	2.35	2.45	2.55	2.55	2.14	2.94	2.55
MnO	0.22	0.19		0.03	0.02	0.01	0.02	0.03	0.02	0.04	0.02	0.01	0.03
P ₂ O ₅	0.24	0.21		0.18	0.17	0.14	0.13	0.19	0.15	0.21	0.08	0.09	0.16
LOI	1.37	1.25		8.61	8.97	9.32	9.06	8.92	9.47	8.82	9.06	8.95	10.21
Sum	99.62	99.73		99.66	99.81	99.86	99.92	99.97	99.85	99.93	99.92	99.55	99.93
V ppm	72	80		214	210	165	190	208	178	202	182	89	182
Cr	603	416		1268	702	484	515	745	527	878	644	823	593
Co	46	36		216	274	17	145	135	107	72	10	28	89
Ni	34	36		117	124	110	122	88	110	188	124	137	79
Rb	83	110		14	15	22	18	8	29	17	24	44	23
Cs	3.53	3.41		0.08	2.21	1.93	2.67	1.17	1.64	0.59	3.08	2.27	1.13
Ba	486	525		31	197	167	222	111	137	73	288	377	105
Sr	416	396		194	206	233	255	269	248	190	142	164	141
Ga	20.5	16.7		23.9	23.3	22.8	21.3	24.4	22.4	23.6	18.3	22.8	23.2
Th	7.64	6.84		9.65	16.2	15.11	16.9	12.84	14.04	10.94	17.51	20.2	12.59
U	2.82	2.73		4.55	7.65	11.25	8.6	8.9	9.65	6.62	11.95	11.2	8.2
Cu	56	58		11	9	8	11	12	11	10	7	8	11
Y	48.3	46.5		61.1	65.4	61.6	60.6	62.9	58.1	59.1	55.6	44.4	58.6
Zr	241	238		271	306	322	284	294	297	285	258	333	290
Ta	0.4	0.5		0.7	1.7	1.4	1.6	1.4	1.2	0.9	1.6	2.3	1.5
Nb	30.7	33.8		46.5	46.4	38.9	45.4	41.2	41.4	45.3	38.4	41.5	47.2
Hf	5.4	5.9		9.9	9.5	8.9	8.9	9.4	8.3	9.7	8.4	10.3	9.4
La ppm	57.4	50.9		68.4	62.4	64.8	68.4	64.8	67.2	65.7	70	68	64.2
Ce	93.7	71.4		174.2	155.6	154	142.1	162.4	152.4	165.2	137.5	151	160.2
Pr	6.13	7.22		12.64	13.35	13.05	13.85	12.45	12.76	11.50	14.8	11.02	12.2
Nd	27.5	24.6		65.2	50.1	49.3	52.1	46.8	48.8	51.6	54.9	64.2	47.4
Sm	6.24	6.92		18.1	10.4	11.54	10.45	13.74	12.74	14.91	10.55	13.2	11.82
Eu	1.64	2.06		7.88	3.24	3.94	3.12	5.45	4.64	5.65	3.02	4.02	5.145
Gd	8.15	7.06		27.8	11.6	13.89	10.40	18.7	16.18	22.25	9.78	11.4	19.2
Tb	1.76	1.84		1.45	1.57	1.44	1.48	1.49	1.42	1.47	1.42	3.21	1.42
Dy	11.24	12.62		9.21	9.11	8.6	8.10	7.45	7.22	8.45	7.40	6.92	6.88
Ho	3.6	3.7		2.41	1.54	1.65	1.47	1.87	1.71	2.13	1.43	2.11	1.98
Er	5.87	5.98		3.97	4.22	4.24	4.45	4.12	4.45	4.02	4.90	3.78	4.18
Tm	0.96	0.89		0.68	0.51	0.45	0.54	0.62	0.59	0.63	0.61	0.41	0.61
Yb	8.9	9.91		5.64	4.01	4.21	3.84	4.74	4.41	5.07	3.63	5.2	4.71
Lu	0.88	0.85		0.64	0.58	0.56	0.55	0.49	0.54	0.59	0.54	0.49	0.54

Geology

The most important rock units in the study area from oldest to the youngest include formations such as Precambrian shale, dolomite, and limestone; Cambro-Ordovician sandstone, carbonate, and shale (Mila F.); Lower Permian sandstone, shale, and diabase (Dorud F.); Middle

to Late Permian carbonates (limestone and dolomite) and diabase (Ruteh F.); Triassic carbonates and andesite (Elika F.); Jurassic sandstone, shale, mudstone, and siltstone (Shemshak F.); Cretaceous sandstone, limestone and shale; Miocene limestone, conglomerate, and volcanics (Qom F.); and Plio-Quaternary

conglomerates (Fig.1). The conspicuous geological features in the area are the presence of a stratiform and lenticular lateritic horizon within the carbonate rocks (Fig.2) of Ruteh Formation (Middle to Late Permian), and horizon of bauxitic-lateritic-kaolinitic rocks along the contact of dolomites of Elika Formation (Triassic) and sandstones of Shemshak Formation (Jurassic) (Fig.1). The Permian lateritic horizon includes 13 discontinuous layers and lenses showing 3 general trends, NW-SE, NE-SW, and N-S extending 5.3 km, and having thicknesses ranging from 4 to 18 meters. The Permian lateritic ores are in two distinct forms, massive and stratified, and show various colors including red, dark red, brick red, brown, and brownish red. Relative to the stratified, the massive ores are denser and were mainly developed adjacent to the carbonate bedrock. Lateritic ores constitute the large portion of residual system within the layers and lenses. Some of them, however, especially in the upper parts of the horizon due to kaolinization and bauxitization were partially altered to kaolin and bauxite displaying a spectrum of white, pink, Cream, green, and gray colors. The bedrocks of this horizon in most places at the contact with laterites were turned into pink to purple color as the result of gradual diffusion of Fe-bearing solutions into existing interstices. Lateritic ores were occasionally and partially limonitized by oxidizing supergene processes. Non-systematic joints, owing to dynamic stress, were developed into some lateritic layers and lenses. Development of cataclastic texture within the deposit was caused by the activity of faults. The remnants of partially altered diabasic rocks in the form of irregular patches were also observed at the contact of the bedrock with lateritic ores. Furthermore, it seems that the laterites were developed chiefly on the cavities, depressions, and karstic sinkholes of the bedrocks. Other notable geological features in the area include the sharp contact between the lateritic ores and enclosing rocks; the presence of mesoscopically observable ooids and occasionally macro-pisoids in the ores; and the existence of dendritic Mn-oxides and hematitic micro-veinlets in ores. Some ores have soapy, greasy, and earthy feels while others are hard and massive with conchoidal fracture surfaces.

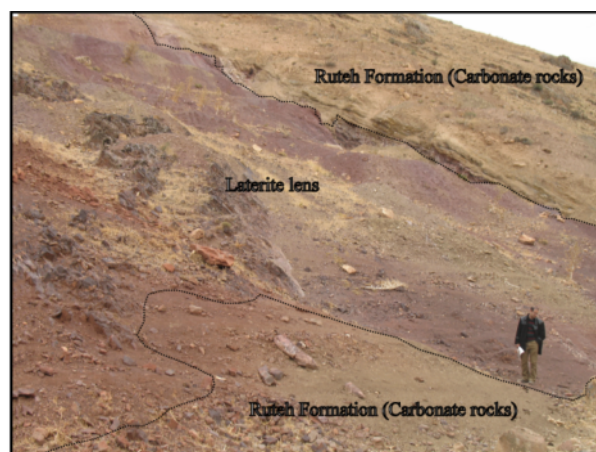


Fig.2 A field photograph of a lateritic lens developed within carbonate rocks of Ruteh Formation. View toward northeast.

Petrography

Petrographic examinations show that texture-forming units in the lateritic ores include pelitomorphic and micro-granular matrix; concentric features such as micro-ooids, pisoids, spastoids, and macro-pisoids (Fig.3a); and films and coatings on pre-existing minerals, nodules, concretions, and filled interstices. In thin-polished sections, hematite is the only identifiable mineral which occurs frequently as nucleus in ooids, pisoids, spastoids, and macro-pisoids, and also occasionally forms alternate concentric bands around the nucleus. The concentric bands around nucleus rarely exceed 6. Hematites within the ores are in four different forms including nodular, acicular (Fig.3b), micro-veinlet (Fig.3c), and banded (Fig.3d). The nodules vary in diameter from 3 to 10 mm, and have more or less spherical to elliptical shape occasionally showing weak orientation within the matrix. Their diameter increases at the proximity of the bedrock. There are some macro-pisoids in the lateritic ores which enclose micro-ooids and ooids (Fig.3e). Occasionally, some pisoids along with their matrix have suffered fracturing (Fig.3f).

Mineralogy

X-ray Diffraction (XRD) analyses demonstrated that the lateritic ores have rather simple mineralogy (Fig.4). The major ore-forming minerals in order of abundance are hematite (44.34%), boehmite (20.44%), kaolinite (20.40%), goethite (4.10%), diasporite (3.26%), illite (2.70%), rutile (2.50%), montmorillonite (1.70%), and chlorite (0.56%) (see table 1). There is a negative

correlation between Fe-bearing minerals (e.g., hematite and goethite) and clays (e.g., kaolinite, montmorillonite, chlorite, and illite) in the lateritic ores (Fig.5). Plotting of semi-quantitative values of the ore-forming minerals on trivariate diagram [7]

(Fig.5) illustrates that the lateritic ores consist of four mineralogic types, (1) aluminous ferrite, (2) kaolinitic laterite, (3) ferritic laterite, and (4) siliceous ferrite (Fig.6).

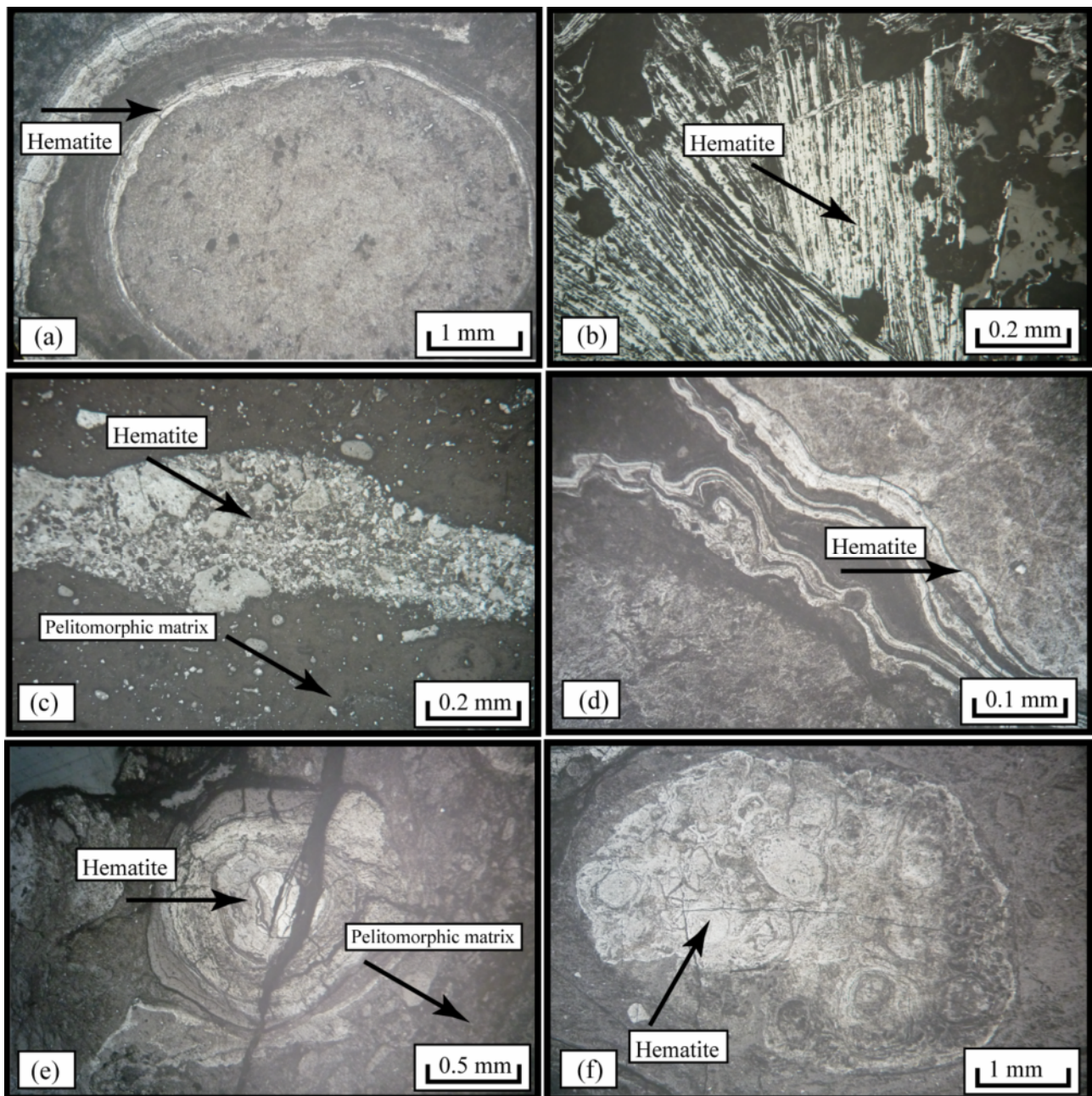


Fig.3 Photomicrographs (XPL) of the lateritic ores at study area. (a) Macro-pisoids with hematitic bands around the nucleus. (b) Development of acicular hematite in the ore matrix. (c) Hematitic micro-veinlets within the pelitomorphic matrix. (d) Occurrence of banded hematite. (e) Development of pisoids with hematitic nucleus within a pelitomorphic matrix. (f) The presence of composite micro-ooids and ooids as nucleus within a macro-pisoid suggesting a polycyclic nature for the ores.

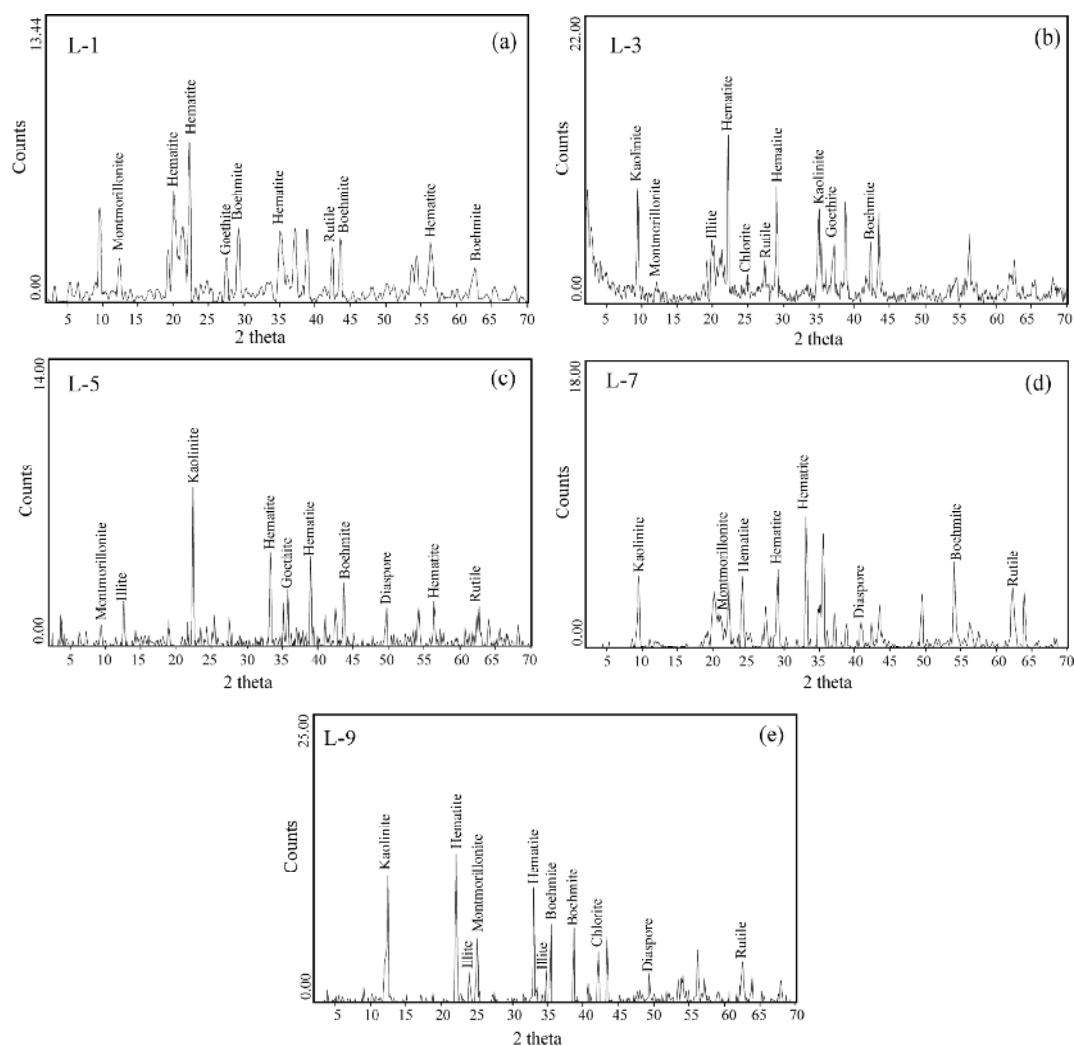


Fig.4 XRD patterns of laterite samples: (a) L1 (hematite, boehmite, goethite, rutile, and montmorillonite); (b) L3 (hematite, kaolinite, boehmite, goethite, rutile, illite, montmorillonite, and chlorite); (c) L5 (hematite, kaolinite, boehmite, diaspore, goethite, rutile, illite, and montmorillonite); (d) L7 (hematite, boehmite, kaolinite, ruile, diaspore, and montmorillonite); (e) L9 (hematite, kaolinite, boehmite, illite, montmorillonite, diaspore, ruile, and chlorite).

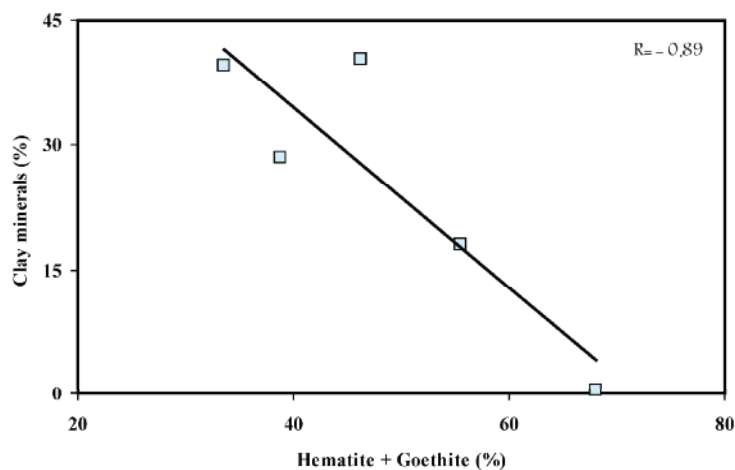


Fig.5 Relationship between distribution of clay and Fe-bearing minerals within the lateritic ores at studied area.

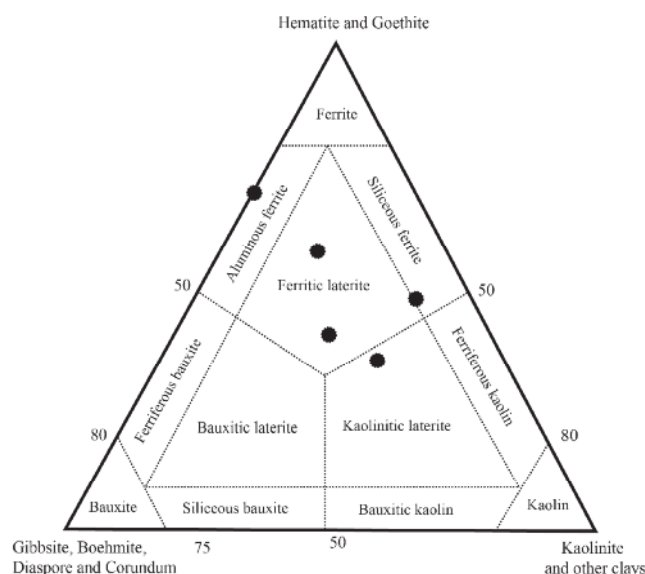


Fig.6 Position of data points of the lateritic ores at studied area on a trivariate plot of Fe-bearing minerals (hematite and goethite), clays (kaolinite and other clays), and free aluminum (gibbsite, boehmite, diaspore, and corundum) [7].

Chemistry of major elements and classification of ores

Chemical analyses show that the total values of Fe_2O_3 , Al_2O_3 , and SiO_2 in the lateritic ores range, in general, from 85.5 to 88.1 wt%. These values are used for classification of the ores. Plotting of these three components on a trivariate diagram presented by Aleva [8] illustrates that the ores can be classified in three general groups, (1) laterite, (2) ferritic laterite, and (3) bauxitic ferrite (Fig.7).

Discussion

Genetic aspects of lateritization inferred from field and laboratory data

Development of the lateritic ores in pits, depressions, and sinkholes of carbonate bedrocks clearly implies that draining of surface waters was the basic parameter controlling the intensity of lateritization in the area. The existence of sharp contact between the bedrocks and lateritic horizon indicates that the parent rocks of the ores were quite independent from carbonate bedrocks. The development of concentric components such as macro-pisoids, micro-ooids, ooids, and pisoids within the ores is indicative of the effective role of diagenetic processes during lateritization [7]. Diasporization of boehmite and formation of rutile can be related to factors such as diagenesis and function of epigenetic processes (burial pressure) on this deposit [1]. The presence of ooids and micro-ooids in nucleus of macro-pisoids suggests a polycyclic nature for the formation of the lateritic ores. The weak orientations in distribution of

nodules and development of filled interstices in the matrix testify that the ores suffered somehow tectonic deformation.

According to D'Argenio and Mindszenty [9], depositional environments for this type of ores can be summarized in two terms, vadose and phreatic. Both matrix and ooids in the residual ores related to vadose environments, owing to its oxidizing nature, normally have rather abundant hematite and goethite accompanied by lesser amounts of boehmite. The residual ores related to phreatic environments, however, are less oxidizing and rather depleted in Fe^{3+} and hence have paler colors. The principal Fe-minerals in phreatic zone are goethite, siderite, pyrite, and \pm chlorite (chiefly chamosite which are accompanied by Al-bearing minerals (e.g., diaspore and boehmite) [9]. Based upon mineralogy and petrographic characteristics of the ores, it seems the laterites in east of Shahindezh were developed in a vadose environment.

Geochemistry of mass changes

Until now, various methods have been employed for consideration of behavior of elements in the course of weathering by many researchers including volume factor method [10], isocon method [11], and method of immobile element [12-17]. In this study, for calculation of the degree of depletion and enrichment of elements during evolution of the lateritic ores, the method presented by van der Weijden and van der Weijden [17],

which is based upon composition of protolith and normalization of geochemical data, was used.

1- protolith: The presence of patches of remnants of partially altered mafic igneous rocks at the proximity of the contact of the lateritic ores with the carbonate bedrocks and also the sharp boundaries of weathered horizon with its enclosing rocks provide reasons to believe that the ores are intimately and genetically affiliated to these diabasic rocks. Petrographic investigations done by Abedini [5] demonstrated that the diabasic rocks in the area have ophitic and micro-granular textures and mineralogically consist of feldspars (plagioclase and K-feldspar), ferromagnesian minerals (olivine, augite, and amphibole), opaque minerals (pyrite and ilmenite), and accessory minerals (apatite and zircon) accompanied by some chlorite and epidote as alteration products.

For consideration of genetic relationship between diabasic rocks and the lateritic ores attempts have been made to compare the weathering products of various protoliths in different parts of the world, and also to utilize the $\text{Al}_2\text{O}_3/\text{TiO}_2$ values, distribution pattern of REEs, and geochemistry of immobile elements. Comparison of weathering products of various protoliths from different parts of the world [18] with the lateritic ores of the study area suggests a mafic origin for ores. Hayashi et al. [19] showed that residual ores having $\text{Al}_2\text{O}_3/\text{TiO}_2 < 21$ and $\text{Al}_2\text{O}_3/\text{TiO}_2 > 21$ belong to mafic and felsic

protoliths, respectively. By plotting the Al_2O_3 and TiO_2 values of the lateritic ores on the bivariate diagram of Al_2O_3 - TiO_2 , it has become evident that the studied ores most likely are the product of weathering and alteration of mafic igneous rocks (Fig.8). Consideration of distribution pattern of REEs normalized to chondrite [20] revealed a weak differentiation of LREEs from HREEs and also a negative Eu anomaly during lateritization (Fig.9). Felsic igneous rocks commonly are favored with strong differentiation of LREEs from HREEs and striking negative Eu anomalies during weathering processes, whereas the differentiation and negative Eu anomalies are weak for ores of mafic origin [21-22]. It appears the distribution pattern of REEs in the study area to be compatible with mafic protolith. Studies done by Valeton et al. [23] showed that Zr and TiO_2 remain immobile during weathering processes and are favorable for determination of the lateritic precursor. Zr- TiO_2 plot for the lateritic ores of the study area exhibits a positive correlation (0.92), and the data point of diabasic rocks also lies on the line of weathering (Fig.10). This may confirm the genetic relationship between the ores and the diabasic rocks. Therefore, the diabasic patches, existing at the proximity of the contact between the ores and the carbonate bedrocks, are the best candidates as protolith for the ores in this area.

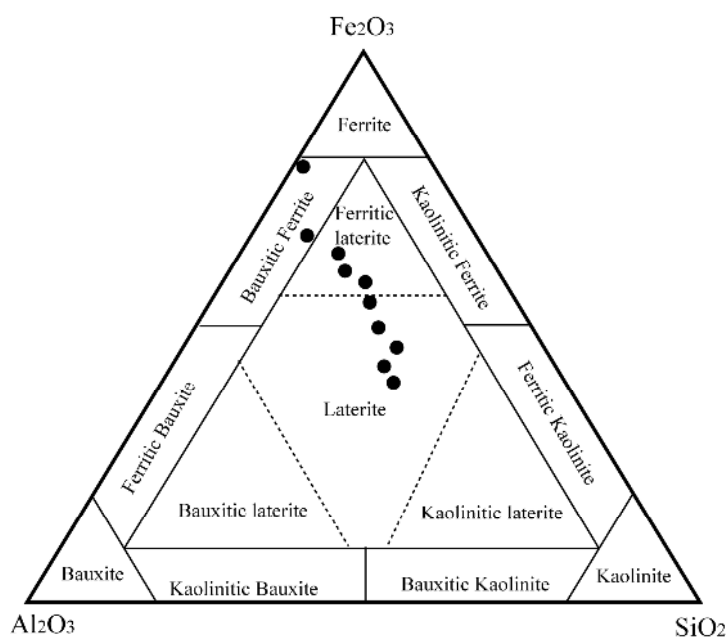


Fig.7 Position of data points of the lateritic ores at studied area on a trivariate plot of Al_2O_3 - Fe_2O_3 - SiO_2 [8].

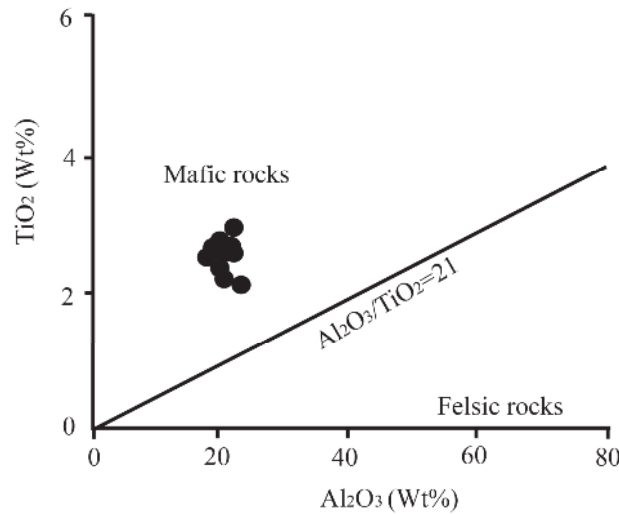


Fig.8 Position of data points of the lateritic ores at studied area on a bivariate plot of Al_2O_3 - TiO_2 . The boundary between felsic and mafic ($\text{Al}_2\text{O}_3/\text{TiO}_2 = 21$) is from [19].

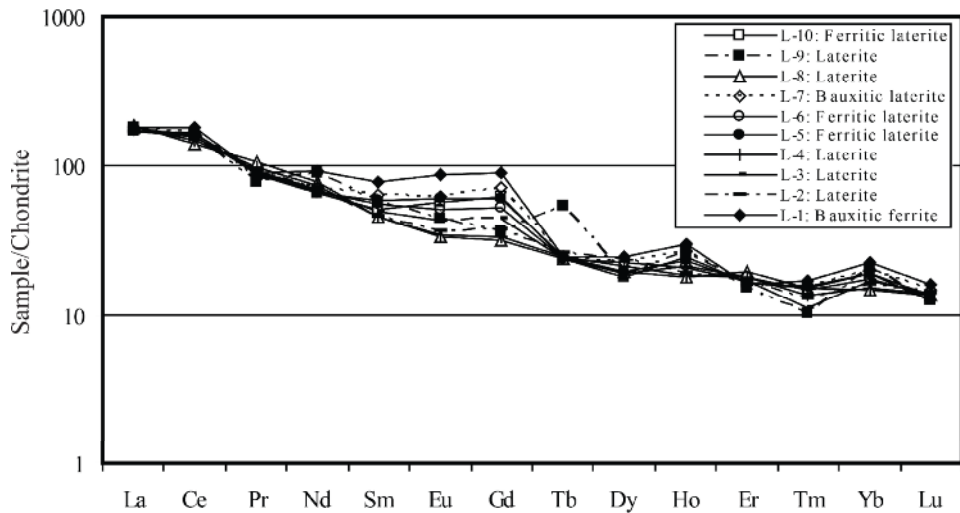


Fig.9 Distribution pattern of REEs normalized to chondrite [20] in the lateritic ores at studied area.

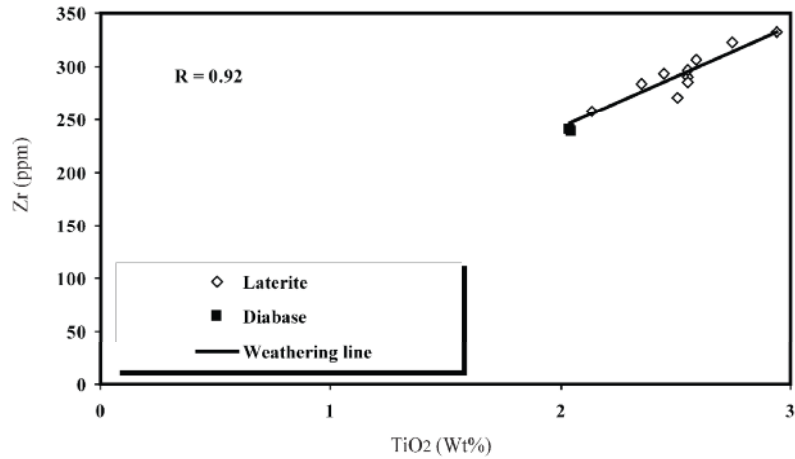


Fig.10 A bivariate plot of TiO_2 -Zr in the lateritic ores at studied area. Noticeable on this figure is the data points of diabasic rocks that lie on the line of weathering.

2- Normalization of geochemical data and calculations of mass changes of elements:

According to van der Weijden and van der Weijden [16], after determination of protolith the requisite for implementing mass changes of elements during lateritization is to select two appropriate elements with least variability among immobile elements (e.g., Nb, Nd, Th, Hf, Zr, Ti, Al) as a basis for calculations. In this study, Zr and Th were chosen as appropriate immobile elements for calculations of $F_{(Th+Zr)}$ (enrichment factor of conservative elements) of the ores by using the following equation:

$$F_{(Th+Zr)} = [(0.1 \times (Th + Zr)_{\text{protolith}}) / [0.1 \times (Th + Zr)_{\text{laterite}}]]$$

Then the mass changes (loss and gain) of elements can be quantitatively calculated by applying the following equation:

$$\% \text{ Change} = 100 \times [F_{(Th+Zr)} \times (X_{\text{laterite}} / X_{\text{protolith}})]$$

The obtained results from the calculations of mass changes for three types of the ores (laterite, ferritic laterite, and bauxitic laterite) are illustrated in the form of increase-decrease for major, minor, trace, and earth elements as well as for LOI (Figs. 10, 11, 12). It is worthy to be noted that there are possibilities for analytical errors as well as for heterogeneity in protolith composition. Therefore, a range of -20% to +20% was regarded as limits of uncertainty, and for interpretation of the results only values out of this range were considered to be the basis for mass gain or loss. By referring to the obtained results (see Figs. 11, 12, 13), it has been manifested that elements such as Si, Na, K, Mg, P, Ca, Ba, Rb, Sr, Cs, Cu, and HREE (Tb-Lu) were leached and elements such as Fe, V, Cr, Ni, Co, U, Ta, Nb, Hf, Ce, Pr, Nd, Sm, Eu, Gd and as well as LOI were enriched during the evolution of the lateritic ores. Al, Ti, Ga, Y, and La lie within the uncertainty limit and hence most likely should have acted as immobile elements during lateritization.

Effective factors in mobility, distribution, and behavior of elements during lateritization

Major and minor elements and LOI: Because of having invariable oxidation state and high ionic potential, Al and Ti ions are commonly can hardly ever be transported by weathering solutions [24]. Based on mineralogy of the protolith (diabase), Al of the lateritic system is derived from alteration of feldspars and Ti from the decomposition of ferromagnesian silicates and ilmenite [25]. Depletion of Si from the system is due to both

kaolinization and subsequent lateritization. Enrichment of Fe during lateritization is caused by the consumption of H^+ of downward-percolating weathering solutions by carbonate bedrocks. Iron of the residual system was derived from break down of pyrite, ilmenite, and ferromagnesian silicates [26]. In general, elements like K, Na, Ca, Mg, Mn, and P suffered depletion (mass loss) owing to destruction of feldspars (K, Na, and Ca), to decomposition of ferromagnesian minerals (Mg and Mn), and to break down of apatite (P) of the protolith during lateritization. Enrichment of LOI is indicative of the development of hydrous mineral phases during lateritization.

Trace elements: The relative similarity in the mode of enrichment of elements such as Cr, V, Co, Nb, and Hf and somewhat Ni and U (Fig.12) to that of Fe (Fig.11) may indicate that these elements were enriched within the system by various mechanisms like isomorphic substitution, simultaneous sorption and/or deposition, and incorporation with Fe-oxides and-hydroxides [27]. It looks that the partial egress of Sr, Cs, Ba, Cu, and Rb (Fig.12) from the system was performed by the alteration of feldspars in the course of water-rock interactions. The good and positive linear correlation of K with Rb ($R = 0.72$), Cs ($R = 0.83$), and Ba ($R = 0.99$) testifies that the distribution of these elements in the ores was controlled mainly by illite. Rather similar mode of variations of Ga and Y (Fig.12) to that of Al (Fig.11) may serve as evidence for the effective role of clay minerals, diaspore, and boehmite in fixing these elements within the ores [28]. Although a particular similarity for the mode of enrichment of Ta with most of major and minor elements is not observed, a good and positive correlation exists between Ta and Al ($R = 0.71$) that may attest to its adsorption by clay minerals as an important mean for fixation and enrichment of Ta within the ores [27].

Rare earth elements: Except La, enrichment of REEs and depletion of HREEs during lateritization in the study area are related to two parameters, (1) pH and (2) degree of stability of complexing ligands in the ore-forming solutions. The low and high pHs cause leaching and enrichment of REEs during lateritization processes, respectively [29]. By considering the enrichment of Fe during formation of the lateritic ores, it can be deduced that the enrichment of REEs is somehow related to the high pH of the system which, in turn, is related to the function of carbonate bedrocks as an active buffer. Normally, the scavengers such as Fe-

oxides and-hydroxides better act for absorption of REEs in high pH environments [30]. It is most likely the function of such mechanism was very effective in fixing and enriching of REEs in the course of lateritization. Since the pH of environment during the formation of the lateritic

ores in the study area was high (due to buffering of weathering solutions by carbonate bedrocks), formation of carbonate-HREE complexes can be regarded as the only logical reason for leaching HREEs from the system [31-32].

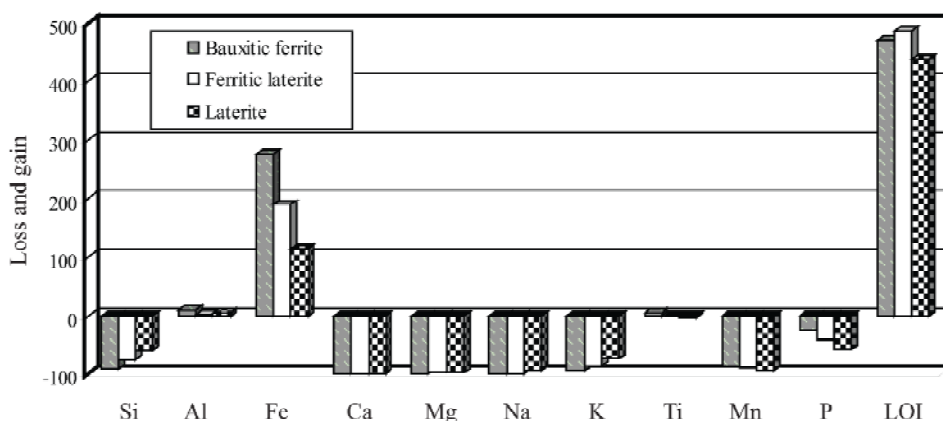


Fig.11 Mass changes for major, and minor elements as well as LOI during the formation of various lateritic types at studied area.

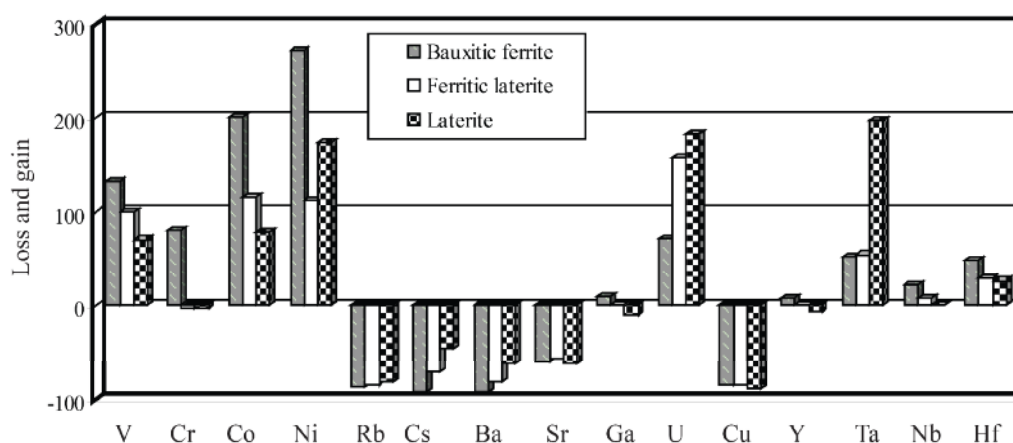


Fig.12 Mass changes for trace elements during the formation of various lateritic types at studied area.

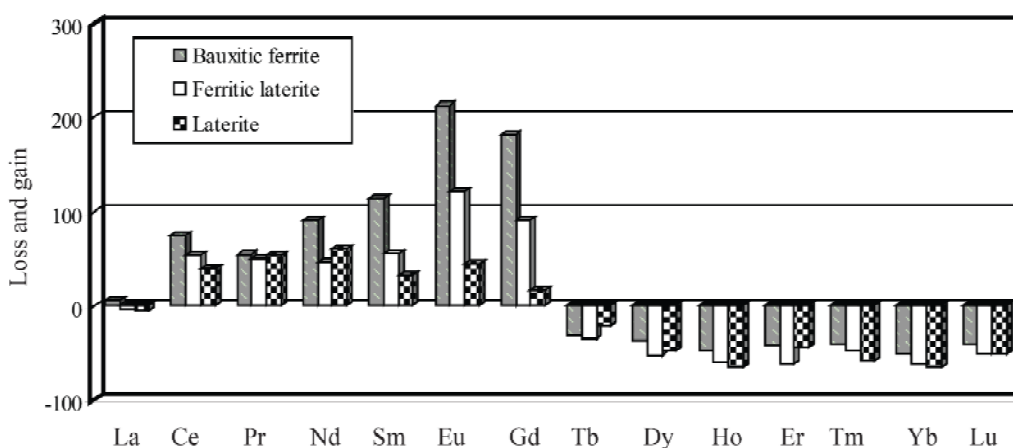


Fig.13 Mass changes for rare earth elements (REE) during the formation of various lateritic types at studied area.

Physico-chemical conditions of the environment of formation of the lateritic ores

In this study, for consideration of physico-chemical conditions of the environment the following equations have been applied for the calculations of $(\text{LREE}/\text{HREE})_p$, Eu/Eu^* , and Ce/Ce^* :

$$(\text{LREE}/\text{HREE})_p = [(\text{LREE}/\text{HREE})_{\text{laterite}} / (\text{LREE}/\text{HREE})_{\text{diabase}}]$$

$$\text{Eu}/\text{Eu}^* = (\text{Eu}_{\text{laterite}}/\text{Eu}_{\text{diabase}}) / \sqrt{[(\text{Sm}_{\text{laterite}}/\text{Sm}_{\text{diabase}}) \times (\text{Gd}_{\text{laterite}}/\text{Gd}_{\text{diabase}})]} \quad [20]$$

$$\text{Ce}/\text{Ce}^* = (2\text{Ce}_{\text{laterite}}/\text{Ce}_{\text{diabase}}) / [(\text{La}_{\text{laterite}}/\text{La}_{\text{diabase}}) + (\text{Pr}_{\text{laterite}}/\text{Pr}_{\text{diabase}})] \quad [33]$$

The obtained results demonstrated that the range of values for $(\text{LREE}/\text{HREE})_p$, Eu/Eu^* , and Ce/Ce^* in ores are 2.64-3.67, 1.19-1.40, and 1.24-1.74, respectively (table 3). The increase of the variation range of $(\text{LREE}/\text{HREE})_p$ from 2.64 to 3.67 indicate coupled differentiation and enrichment of LREEs relative to HREEs during lateritization processes. What can be deduced from this variation range is that the pH of the environment in which the ores were developed was alkaline. In surficial environments with alkaline pHs, the complexes of HREEs are more stable than that of LREEs [34]. It looks that the rise of underground water table in carbonate bedrocks brought about a pH increase in the weathering solutions which, in turn, caused enrichment of LREEs and leaching of HREEs in the ores. Since behavior of Ce during weathering processes severely depends on pH and Eh variations [35], the positive Ce anomaly in the ores is likely due to the scavenging of Ce by Fe-oxides and-hydroxides [36-37]. It appears that this process occurred in relation to Eh variation of the environment, fluctuation of underground water table [38], and pH increase of drained waters by carbonate bedrocks [35]. By taking the mass increase of iron into account, it can be inferred that the creation of positive Eu anomaly is related to direct deposition of iron and its variation also is controlled by the same mechanism that controlled the iron deposition during lateritization.

Table 3 Values of $(\Sigma\text{LREE}/\Sigma\text{HREE})_p$ and anomalies of Eu and Ce in the lateritic ores in studied area.

	L-1	L-2	L-3	L-4	L-5	L-6	L-7	L-8	L-9	L-10
$(\Sigma\text{LREE}/\Sigma\text{HREE})_p$	2.89	2.64	2.72	2.72	2.89	2.86	2.79	2.79	2.70	3.67
Eu/Eu*	1.42	1.19	1.29	1.23	1.40	1.32	1.27	1.22	1.36	1.40
Ce/Ce*	1.69	1.58	1.54	1.32	1.64	1.74	1.69	1.24	1.54	1.64

Conclusion

The significant results acquired from mineralogical and geochemical studies of the lateritic ores at east of Shahindezh are as follows:

1- By taking the semi-quantitative values of hematite, boehmite, kaolinite, diasporite, goethite, montmorillonite, illite, chlorite, and rutile into account, the ores on the basis of mineral type in the study area can be categorized into four distinct facies, (1) aluminous ferrite, (2) kaolinitic laterite, (3) ferritic laterite, and (4) siliceous ferrite.

2- Consideration of the chemistry of major elements indicates that the studied ores belong to three rock types, (1) bauxitic ferrite, (2) laterite, and (3) ferritic laterite.

3- Geochemical indices such as low degree of segregation of LREEs from HREEs, creation of weak negative Eu anomaly, values of $\text{Al}_2\text{O}_3/\text{TiO}_2$ and geochemistry of immobile elements show that the ores were produced by the weathering and alteration of diabasic rocks existing in the area.

4- By combining the obtained mineralogical and analytic mineralogical data indicate that diagenetic and epigenetic processes played crucial roles in evolution of the ores, and that the lateritization occurred in an almost vadose environment.

5- Chemical characteristics of elements, consumption of H^+ of the downward-permeating weathering solutions by the carbonate bedrocks, and also the development of neomorph hydrous mineral phases played important roles in controlling the behavior and distribution of major and minor elements and LOI during the formation of the lateritic ores.

6- Various mechanisms like isomorphic substitution, adsorption, contemporaneous deposition, degree of resistance of primary minerals against weathering, incorporation in crystal structure, and mineralogical control were the most important factors governing the distribution of trace elements in the course of lateritization.

7- The pH increase of weathering solutions caused by buffering of carbonate bedrocks was the important parameter in scavenging of REEs by Fe-oxides and-hydroxides, formation of stable complexes of carbonate-HREEs, and leaching of HREEs during lateritization.

8- Geochemical studies demonstrate that the occurrence of Eu and Ce anomalies in the ores are in relation to the Eh variation of the environment,

fluctuation of underground water table, and pH increase of the drained waters by carbonate bedrocks.

References

- [1] Bardossy G., "Karst bauxites", Elsevier Scientific, Amsterdam, (1982) 441p.
- [2] Alavi-Naini M., Hajian J., Amidi A., Bolurrchi H., "Geology of Tekab-Saein Qale: Explanatory note of 1:250000 map of Takab guardrangle" Geological Survey of Iran, Report No 50 (1982).
- [3] Kholghi Khasraghi M.H., Eghlimi B., Amini Azar R., "1:100000 map of Shahindezh", Geological Survey of Iran (1994).
- [4] Etemadi S., "Investigation of economic geology of 1:100000 map of Shahindezh", unpublished MSc Thesis (in Persian), Geology Department, Shahid Beheshti University (1997) 170p.
- [5] Abedini A., "Investigations of mineralogy, geochemistry and genesis of the Permian to Triassic bauxitic- lateritic deposits in northwest of Iran", unpublished Ph.D. Thesis (in Persian), Geology Department, Tabriz University (2008) 184p.
- [6] Abedini A., Calagari A.A., Hadjalilu B., "Geological-mineralogical characteristics and trace elements geochemistry in Aghadjari bauxite deposit, south of Shahindezh, NW of Iran (in Persian)", Iranian Journal of Crystallography and Mineralogy 16 (2008) 327-341.
- [7] Bardossy G.Y., Aleva G.Y.Y., "Lateritic bauxites", Akademia, Kiado Budapest, (1990) 646p.
- [8] Aleva G.J.J., "Laterites: Concepts, geology, morphology and chemistry", ISIRC, Wageningen, (1994) 169p.
- [9] D'Argenio B., Mindszenty A., "Bauxites and related paleokarst: Tectonic and climatic event markers at regional unconformities", Eclogae geologicae Helvetiae 88 (1995) 453-499.
- [10] Gresens R.L., "Composition-volume relationships of metasomatism", Chemical Geology 2 (1967) 47-55.
- [11] Grant, J.A., "The isocon diagram: A simple solution to Gresens equation for metasomatic alteration", Economic Geology 81 (1986) 1976-1982.
- [12] Nesbitt H.W., "Mobility and fractionation of rare earth elements during weathering of a granodiorite", Nature 279 (1979) 206-210.
- [13] MacLean W.H., Kranidiotis P., "Immobile elements as monitors of mass transfer in hydrothermal alteration: Phelps Dodge massive sulfide deposit, Matagami, Quebec", Economic Geology 82 (1987) 951-962.
- [14] MacLean W.H., "Mass change calculations in altered rock series", Mineralium Deposita 25 (1990) 44-49.
- [15] Brimhall G.H., Chadwick O.A., Lewis C.J., Compson W., Williams I.S., Danty K.J., Dietrich W.E., Power M.E., Hendricks D., Bratt J., "Deformational mass transfer and invasive processes in soil evolution", Science 255 (1991) 695-702.
- [16] van der Weijden C.H., van der Weijden R.D., "Mobility of major, minor and some redox-sensitive trace elements and rare-earth elements during weathering of four granitoids in central Portugal", Chemical Geology 125 (1995) 149-167.
- [17] Nesbitt H.W., Markovics G., "Weathering of granodioritic crust, long-term storage of elements in weathering profiles, and petrogenesis of siliciclastic sediments", Geochimica et Cosmochimica Acta 61 (1997) 1653-1670.
- [18] Nesbitt H.W., Wilson R.E., "Recent chemical weathering of basalts", American Journal of Science 292 (1992) 740-777.
- [19] Hayashi K., Fujisawa H., Holland H.D., Ohmoto H., "Geochemistry of sedimentary rocks from northeastern Labrador, Canada", Geochimica et Cosmochimica Acta 61 (1997) 4115-1437.
- [20] Taylor S.R., McLennan S.M., "The continental crust: Its composition and evolution", Blackwell. Oxford (1985) 312p.
- [21] Cullers R.L., Graf J., "Rare earth elements in igneous rocks of the continental crust: Intermediate and silicic rocks, ore petrogenesis", In: Henderson, P. (Ed.), Rare Earth Element Geochemistry. Elsevier, Amsterdam, (1983) 275-312.
- [22] Nyakairu G.W.A., Koeberl C., "Mineralogical and chemical composition and distribution of rare earth elements in clay rich sediments from Central Uganda", Geochemical Journal 35 (2001) 13-28.
- [23] Valetton I., Biermann M., Reche R., Rosenberg F., "Genesis of nickel laterites and bauxites in Greece during the Jurassic and Cretaceous, and their relation to ultrabasic parent rocks", Ore Geology Reviews 2 (1987) 359-404.
- [24] Etame J., Gerard M., Bilong P., Suh C.E., "Behaviour of elements in soils developed from nephelinites at Mount Etinde (Cameroon): Impact of hydrothermal versus weathering processes", Journal of African Earth Sciences 54 (2009) 37-45.

- [25] Deer W.A., Howie R.A., Zussmann J., *"The rock forming minerals"*, Longman, London, (1992) 720 p.
- [26] Hill I.G., Worden R.H.G., Meighan I.G., *"Geochemical evolution of a paleolaterite: The interbasaltic formation, northern Ireland"*, Chemical Geology 166 (2000) 65-84.
- [27] Fernandez-Caliani J.C., Cantano M., *"Intensive kaolinization during a lateritic weathering event in southwest Spain: Mineralogical and geochemical inferences from a relict paleosol"*, Catena 80 (2010) 23-33.
- [28] MacLean W.H., Bonavia F.F., Sanna G., *"Argillite debris converted to bauxite during karst weathering: Evidence from immobile element geochemistry at the Olmedo deposit, Sardinia"*, Mineralium Deposita 32 (1997) 607-616.
- [29] Patino L.C., Velbel M.A., Price J.R., Wade J.A., *"Trace element mobility during spheroidal weathering of basalts and andesites in Hawaii and Guatemala"*, Chemical Geology 202 (2003) 343-364.
- [30] Karadag M., Kupeli S., Arik F., Ayhan A., Zedef V., Doyen A., *"Rare earth element (REE) geochemistry and genetic implications of the Mortas bauxite deposit (Seydisehir/Konya-southern Turkey)"*, Chemie der Erde-Geochemistry 69 (2009) 143-159.
- [31] Cantrell K.J., Byrne R.H., *"Rare earth element complexation by carbonate and oxalate ions"*, Geochimica et Cosmochimica Acta 51 (1987) 597-605.
- [32] Johannesson K.H., Stetzenbach K.J., Hodge V.F., Lyons W.B., *"Rare earth element complexation behavior in circum neutral pH groundwaters: Assessing the role of carbonate and phosphate ions"*, Earth and Planetary Science Letters 139 (1996) 305-319.
- [33] Ma J., Wei G., Xu Y., Long W., Sun W., *"Mobilization and re-distribution of major and trace elements during extreme weathering of basalt in Hainan Island, south China"*, Geochimica et Cosmochimica Acta 71 (2007) 3223-3237.
- [34] Muchangos A.C., *"The mobility of rare earth and other elements in process of alteration of rhyolitic rocks to bentonite (Lebombo Volcanic Mountainous Chain, Mozambique)"*, Journal of Geochemical Exploration 88 (2006) 300-303.
- [35] Braun J.J., Pagel M., Muller J.P., Bilong P., Michard A., Guillet B., *"Ce anomalies in lateritic profiles"*, Geochimica et Cosmochimica Acta 54 (1990) 781-795.
- [36] Bao Z., Zhao Z., *"Geochemistry of mineralization with exchangeable REY in the weathering crusts of granitic rocks in south China"*, Ore Geology Reviews 33 (2008) 519-535.
- [37] Sanematsu K., Moriyama T., Sotouky L., Watanabe Y., *"Mobility of REEs in basalt derived laterite at the Bolaven plateau, Southern Laos"*, Resource Geology 61 (2011) 140-158.
- [38] Meyer F.M., Happel U., Hausberg J., Wiechowski T., *"The geometry and anatomy of the Pijigaos bauxite deposit, Venezuela"*, Ore Geology Reviews 20 (2002) 27-54.